

## Simulation and experimental analysis of active vibration control of smart beams under harmonic excitation

L. Malgaca\* and H. Karagülle

*Department of Mechanical Engineering, Dokuz Eylül University, 35100, Bornova / Izmir, Turkey*

(Received May 8, 2007, Accepted July 31, 2008)

**Abstract.** In the present study, active control of a smart beam under forced vibration is analyzed. The aluminum smart beam is composed of two piezoelectric patches and strain gauge. One of the piezoelectric patches is used as controlling actuator while the other piezoelectric patch is used as vibration generating shaker. The smart beam is harmonically excited by the piezoelectric shaker at its fundamental frequency. The strain gauge is utilized to sense the vibration level. Active vibration reduction under harmonic excitation is achieved using both strain and displacement feedback control. Control actions, the finite element (FE) modeling and analyses are directly carried out by using ANSYS parametric design language (APDL). Experimental applications are performed with LabVIEW. Dynamic behavior at the tip of the beam is evaluated for the uncontrolled and controlled responses. The simulation and experimental results are compared. Good agreement is observed between simulation and experimental results under harmonic excitation.

**Keywords:** active control of forced vibration; piezoelectric; finite element analysis.

### 1. Introduction

Active vibration control of smart structures requires developing the mathematical model of the system first. Commercial FE packages such as ANSYS, ABAQUS and MSC/NASTRAN can be used at this stage where closed loop control actions can be incorporated to the model. Commercial control simulation packages such as MATLAB can be used for the control analysis. Different structures, different modeling techniques, and control analyses are investigated by many researchers. Experimental verifications of simulations are also given in some of the studies. The studies considered in this work are summarized in Table 1.

Fariborzi, *et al.* (1997) experimentally developed energy-based control strategy ‘linear coupling control for controlling forced vibrations in flexible structures. Choi, *et al.* (1998) investigated the active control of two hybrid smart structures under forced vibrations. Bruant, *et al.* (2001) modeled piezoelectric smart beam structures using the FE method with six mechanical and four electric DOFs. Gabbert, *et al.* (2002) studied the FE simulation and the LQ optimal control of a smart plate. Raja and Sihna (2002) derived the FE formulation and developed a control scheme based on the LQR/independent modal space control method for a composite sandwich beam with bending and shear actuators. Jha and Rower (2002) tested the neural network control under sine wave and white noise

\*E-mail: levent.malgaca@deu.edu.tr

Table 1 Smart structures, modeling techniques and control analyses used in the literature

Authors (year)	Smart Structure	Modeling Technique	Control Analysis	Experimental Verification
Fariborzi, <i>et al.</i> (1997)	Beam	Derived	MATLAB	Available
Choi, <i>et al.</i> (1998)	Hybrid	Derived	Developed	Available
Bruant, <i>et al.</i> (2001)	Beam	DYNADID2D	SCILAB	None
Gabbert, <i>et al.</i> (2002)	Plate	COSAR	MATLAB/Simulink	None
Raja and Sinha (2002)	Beam	Derived	Developed	None
Jha and Rower (2002)	Beam	Derived	Developed	Available
Reaves and Horta (2003)	Beam	MSC/NASTRAN	MATLAB	None
Yaman, <i>et al.</i> (2003)	Plate	Derived	Developed	Available
Kusculuoglu, <i>et al.</i> (2004)	Beam	ANSYS and Derived	Developed	Available
Xu and Koko (2004)	Beam and plate	ANSYS	MATLAB/Control system toolbox	None
Karagüllü, <i>et al.</i> (2004)	Beam	ANSYS	ANSYS	None
Baillargeon and Vel (2005)	Beam	ABAQUS	MATLAB/Simulink	Available
Yang and Liu (2005)	Beam <sup>3</sup>	Derived	Developed	Available
Peng, <i>et al.</i> (2005)	Plate	ANSYS	Developed	None
Moita, <i>et al.</i> (2005)	Plate	Derived	Developed	None
Kumar and Singh (2006)	L beam	Derived	MATLAB/Control system toolbox	Available
Seba, <i>et al.</i> (2006)	Beam and chassis frame	ANSYS	MATLAB	Available
Dong, <i>et al.</i> (2006)	Beam	ANSYS	ANSYS	Available
Meng, <i>et al.</i> (2006)	Beam	ANSYS	ANSYS	None
In the present study	Beam	ANSYS	ANSYS	Available

disturbances. MATLAB scripts were used to assemble the dynamic equations after modeling the smart structure by MSC/NASTRAN in Reaves and Horta (2003). Yaman, *et al.* (2003) investigated a  $\mu$  synthesis active vibration control technique applied to the sinusoidal forced vibrations of a smart fin. Kusculuoglu, *et al.* (2004) developed a new FE model for a piezoelectric beam using Timoshenko beam for each layer, and also used ANSYS.

The optimal control design was carried out in the state space form established on FE modal analysis in Xu and Koko (2004). Baillargeon and Vel (2005) studied vibration suppression of adaptive composite smart structures harmonically excited with a stack actuator and used positive position feedback and strain rate feedback control. Yang and Liu (2005) presented a feed forward adaptive controller based on an adaptive filter for system dynamics identification. Peng, *et al.* (2005) developed a performance criterion for the optimization of piezoelectric patch locations with a filtered-x LMS based multi-channel adaptive control. Moita, *et al.* (2005) dealt with a FE formulation for active control of forced vibrations of thin plate/shell laminated structures and obtained the dynamic response by using the Newmark method. Kumar and Singh (2006) studied active control of an inverted piezoelectric L structure under forced vibration and used adaptive hybrid control by combining the feedback and feed forward controllers for a large range of excitation frequencies. Seba, *et al.* (2006) studied vibration attenuation of different smart structures in ANSYS-MATLAB platform for the FE element and control analyses.

As seen from Table 1, the direct control simulation in ANSYS was realized by Karagülle, *et al.* (2004) for the first time. Both the FE modeling and the closed loop control actions in smart structures were achieved in ANSYS environment. This approach makes the active vibration control analyses in smart structures easier. This technique was also used by Dong, *et al.* (2006), Meng, *et al.* (2006), and in this study. Dong, *et al.* (2006) used a state space model developed from experimental results using a modern system identification technique for the purpose of LQG control law design. Meng, *et al.* (2006) used the same technique and control design; however, they developed the dynamic model based on the structure responses determined by the FE method. In this study, the harmonic vibration generating excitation is considered. Displacement feedback in addition to strain feedback is studied. The simulations are verified by experimental results.

## 2. Simulation procedure

Smart structures with metal and piezoelectric sections can be modeled by ANSYS. Three dimensional structural element (SOLID45) is used for the metal part of the smart beam. The piezoelectric patches are modeled using three dimensional coupled elements (SOLID5). The features of the elements used in the analysis, the constitutive equations for the piezoelectric materials and the FE formulation for the coupled field analysis are reviewed briefly.

### 2.1. The finite element background

The element SOLID45 is defined by eight nodes having three degrees of freedom ( $ux$ ,  $uy$ ,  $uz$ ) at each node: translation in the nodal  $x$ ,  $y$ ,  $z$  directions. SOLID5 has a 3D piezoelectric and structural capability between the fields. The element has eight nodes, four degrees of freedom ( $ux$ ,  $uy$ ,  $uz$ , volt) at each node. ANSYS uses the following constitutive equations to model piezoelectric materials (ANSYS 2004).

$$\{T\} = [c]\{S\} - [e]\{E\} \quad (1)$$

$$\{D\} = [e^T]\{S\} + [\varepsilon]\{E\} \quad (2)$$

where mechanical variables  $T$  and  $S$  are stress and strain, respectively; electrical variable  $D$  and  $E$  are electrical displacement and electric field. Matrices  $[c]$ ,  $[e]$ ,  $[\varepsilon]$  are piezoelectric material properties, where  $[c]$  is the elasticity matrix,  $[e]$  is the piezoelectric matrix,  $[\varepsilon]$  is the dielectric matrix. After the application of the variational principle and FE discretization, the coupled FE matrix equation is derived for one element model as follows (Preumont 2002),

$$\begin{bmatrix} M_{uu} & 0 \\ 0 & 0 \end{bmatrix} \begin{Bmatrix} \ddot{u} \\ \ddot{\phi} \end{Bmatrix} + \begin{bmatrix} C_{uu} & 0 \\ 0 & 0 \end{bmatrix} \begin{Bmatrix} \dot{u} \\ \dot{\phi} \end{Bmatrix} + \begin{bmatrix} K_{uu} & K_{u\phi} \\ K_{u\phi} & K_{\phi\phi} \end{bmatrix} \begin{Bmatrix} u \\ \phi \end{Bmatrix} = \begin{Bmatrix} F \\ Q \end{Bmatrix} \quad (3)$$

where,  $[M_{uu}]$  is the mass matrix derived from density and volume,  $[K_{uu}]$  is the mechanical stiffness matrix derived from elasticity matrix,  $[K_{u\phi}]$  is the piezoelectric stiffness matrix, derived from piezoelectric matrix,  $[K_{\phi\phi}]$  is the dielectric stiffness matrix derived from dielectric matrix. The variables  $F$  and  $Q$  are the mechanical force vector and charge vector, respectively. Structural damping matrix  $[C_{uu}]$  is defined as linear combination of mass and mechanical stiffness matrices as follows,

$$C_{uu} = \alpha M_{uu} + \beta K_{uu} \quad (4)$$

where the variables  $\alpha$  and  $\beta$  are the Rayleigh damping coefficients.

## 2.2. Structural modeling

The configuration of the smart beam including two piezoelectric patches and a strain gauge is shown in Fig. 1(a). One of the piezoelectric patches is used as the disturbance generator and it is actuated with a sine wave. The other piezoelectric patch is used as an actuator to control vibrations occurred. The piezoelectric shaker is placed in the middle of the beam. The piezoelectric actuator is 10 mm away from the clamped end. The dimensions of the aluminum beam and the piezoelectric shaker and actuator are  $450 \times 20 \times 1.5$  mm<sup>3</sup>,  $25 \times 20 \times 1$  mm<sup>3</sup> and  $25 \times 20 \times 1$  mm<sup>3</sup> respectively. The strain gauge which is placed 25 mm away from the clamped end at the opposite side of the beam senses the vibration level during the excitation. The material properties of the smart beam are given in Table 2.

The FE modeling of a smart beam with a piezoelectric element is described in the reference (Karagüllü, *et al.* 2004). The FE model for this study is constructed in the file “femodel.txt”. The FE model having 438 elements and 990 nodes is shown in Fig. 1(b). The adhesive part is neglected in the simulation. Cantilever boundary conditions are assumed. Natural frequencies are found with modal analysis using Block-Lanczos solver. Bending modes in the z direction are considered.

In the transient analysis, Rayleigh damping coefficients ( $\alpha$  and  $\beta$ ) must be determined for the structural damping matrix described in Eq. (4). The coefficients ( $\alpha$  and  $\beta$ ) are determined according to the experimental free vibration response of the smart beam. First, the free vibration response under an initial displacement is obtained by the experiment. Then, the free vibration analysis with initial conditions is performed. Coefficients  $\alpha$  and  $\beta$  are determined by inspection so that the experimental and

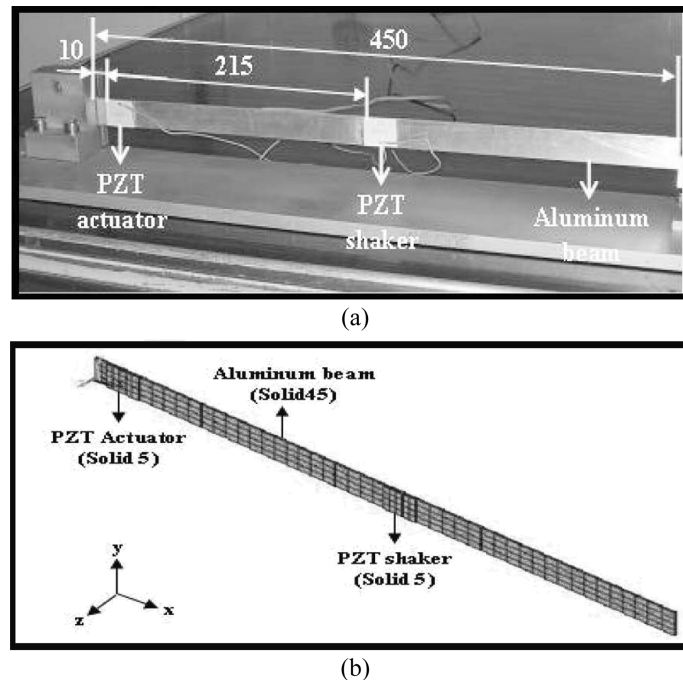


Fig. 1 Smart beam (a) configuration (b) the finite element model

Table 2 Material properties of piezoelectric patches and aluminum beam

Properties	BM532 (PZT-5H)	Aluminum
Young modulus	-	$62 \times 10^9$ (N/m <sup>2</sup> )
Density	7350 (kg/m <sup>3</sup> )	2676 (kg/m <sup>3</sup> )
Poisson's ratio	-	0.32
Elastic stiffness matrix (N/m <sup>2</sup> )		
$C_{11}$	$12.6 \times 10^{10}$	
$C_{12}$	$7.95 \times 10^{10}$	
$C_{13}$	$8.41 \times 10^{10}$	
$C_{33}$	$11.7 \times 10^{10}$	
$C_{44}$	$2.33 \times 10^{10}$	
Piezoelectric strain matrix (C/m <sup>2</sup> )		
$E_{31}$	6.5	
$E_{33}$	23.3	
$E_{15}$	17	
Dielectric matrix (F/m)		
$\varepsilon_{11}$	$1.503 \times 10^{-8}$	
$\varepsilon_{22}$	$1.503 \times 10^{-8}$	
$\varepsilon_{33}$	$1.3 \times 10^{-8}$	

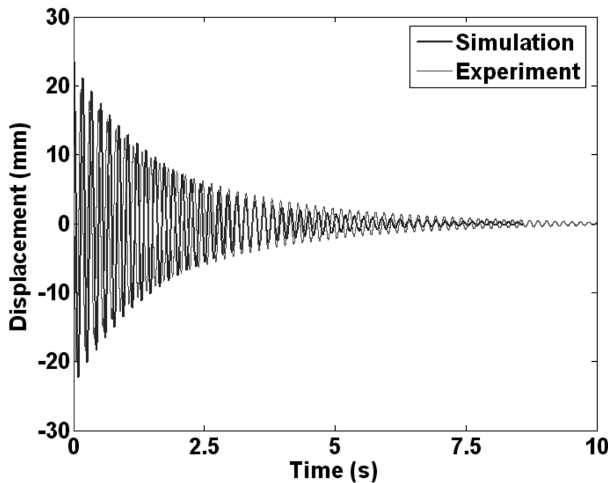


Fig. 2 Free vibration responses under an initial displacement for  $\alpha = 0.0014$ ,  $\beta = 0.0007$

simulation results match. The free vibration responses are shown in Fig. 2. The Rayleigh damping coefficients are taken as  $\alpha = 0.0014$  and  $\beta = 0.0007$  for the simulations.

Harmonic excitation is provided by the piezoelectric vibration generating shaker. The harmonic excitation  $vh = a\sin(2\pi ft)$  is created into the file “Sine.txt” by ANSYS. The amplitude of the excitation ( $a$ ) is 270 V, the frequency of the excitation ( $f$ ) is 6.12 Hz, which is equal to the first undamped natural frequency. The time step is taken as  $\Delta t = 1/f_i/20$ .

### 2.3. Integration of control actions into finite element analysis

The block diagram of the closed loop control is given in Fig. 3. The flowchart of the direct control simulation using commercial FEA software ANSYS is shown in Fig. 4. By using APDL, the analysis of

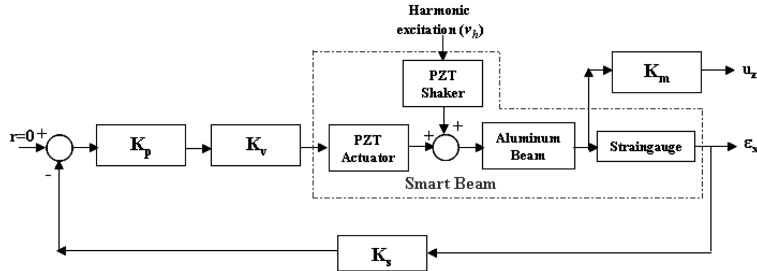


Fig. 3 Block diagram of closed loop control

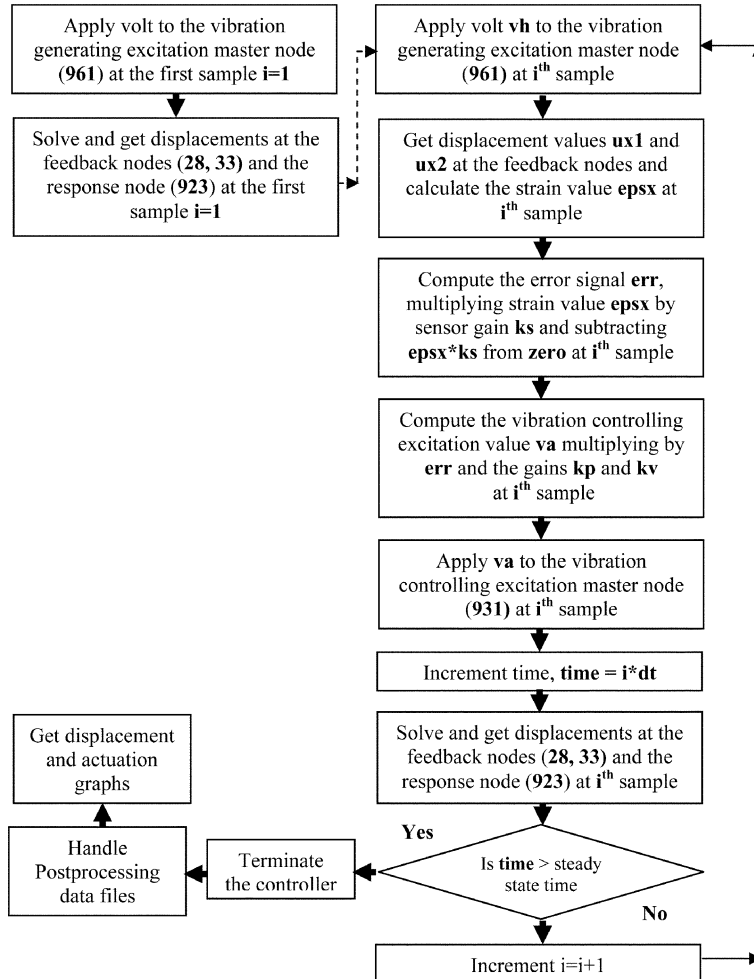


Fig. 4 Flowchart of direct control simulation using ANSYS

active control is carried out with the following scripts.

```
/input,femodel.txt
/input,sine.txt
d,961,volt,vh(1)
time,dt solve
r=0
*do,i,2,ny
d,961,volt,vh(i)
*get,ux1,node,28,u,x
*get,ux2,node,33,u,x
epsx=(ux2-ux1)/dxp
err=r-ks*epsx
va=kp*kv*err
d,931,volt,va
time,i*dt
solve
*enddo
```

The commands in the files “*femodel.txt*” and “*sine.txt*” are performed before the control loop is initiated. The first step is solved applying the excitation voltage (node 961) to the piezoelectric shaker. Therefore, the nodal solutions of the FE model are known for the next step. Active control is realized in “\*do-\*enddo” loop as seen from the flowchart. The excitation is applied again in the first line of the control loop. The elongations *ux1* (node 28) and *ux2* (node 33) known from the first step are read from the nodes corresponding to the strain gauge location. Error signal is obtained after the strain value is calculated. Strain value is multiplied by *ks* to provide optimum control performance. The actuation voltage to be applied for the piezoelectric actuator (node 931) is found multiplying error signal by the gain *k<sub>p</sub>* and *k<sub>v</sub>*. The analysis goes on step by step for a specific duration after vibration amplitudes reach steady-state. The parameter *ks* is taken as 10000 for strain feedback control. The parameter *k<sub>v</sub>* is an amplification factor used in the experiment.

The feedback lines in the control loop are changed for displacement feedback. The displacement feedback signal is obtained with the line “\*get,uz,node,923,u,z”. Displacement *uz* (node 923) is converted to voltage with the line “*vd=km\*uz*”. The parameter *km* is related to laser displacement meter used in the experiment and is taken as 250 V/m. The error signal is calculated with the line “*err=r-vd*”. The response node is the same as the feedback node. For strain and displacement feedback, active control results are obtained using the same controller gains. The uncontrolled and controlled vibration responses with strain and displacement feedback are shown in Fig. 5.

#### 2.4. Experimental setup

Experimental setup is shown in Fig. 6. The smart beam is produced by bonding two piezoelectric patches to the aluminum beam with conductive epoxy. The piezoelectric actuator is placed near the clamped end of the beam to perform effective control as shown in Fig. 1. The piezoelectric shaker placed in the middle of the beam generates harmonic excitation. The ground lines of the two patches are not common. The ground line of the piezoelectric actuator is aluminum beam while that of the

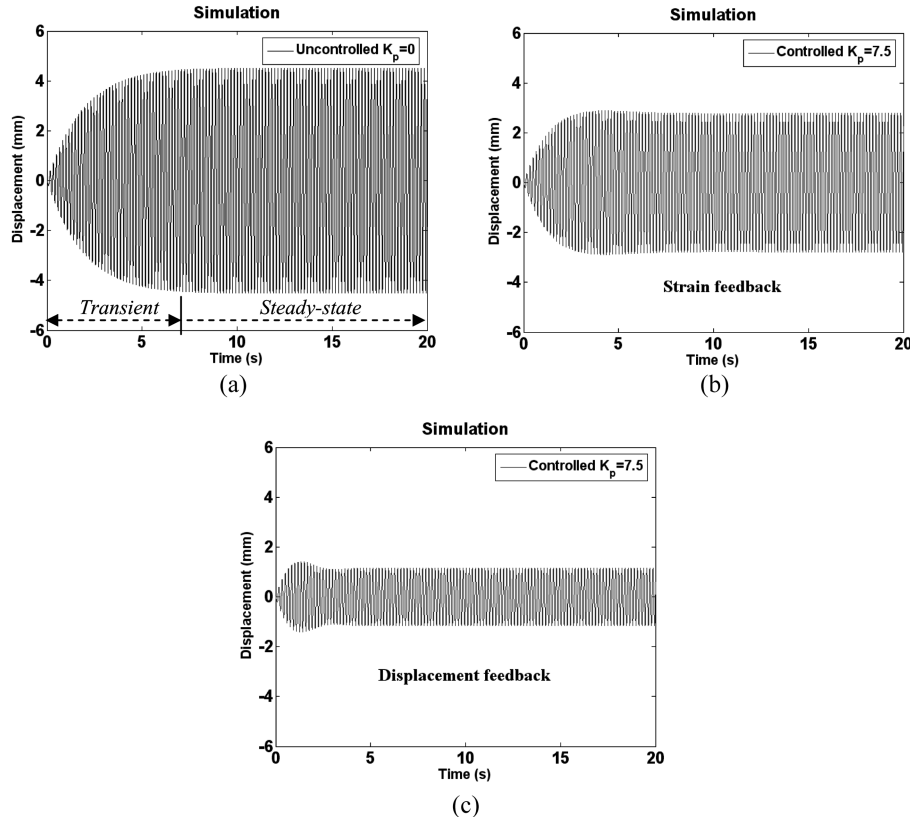


Fig. 5 Simulation results with sine wave of 6.12 Hz (a) uncontrolled response, (b) controlled response with strain feedback for  $K_p=7.5$  (c) controlled response with displacement feedback for  $K_p=7.5$

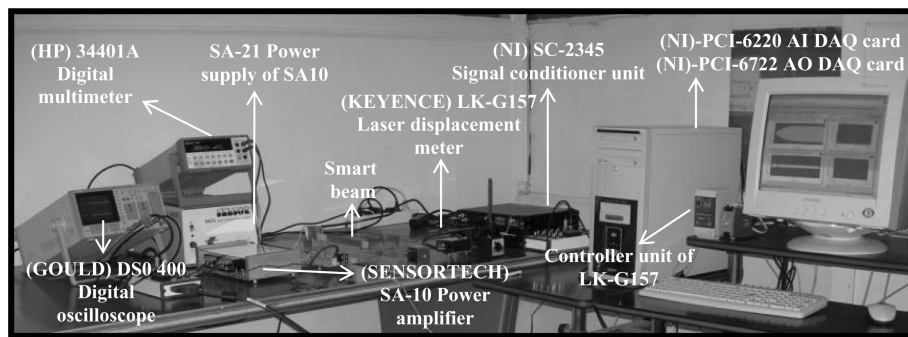


Fig. 6 Experimental setup

piezoelectric shaker is isolated from the beam. The strain gauge which is bonded to the beam at the opposite side of the piezoelectric patches measures the vibration level. The smart beam fastens to a rigid fixture for cantilever boundary conditions. The uncontrolled and controlled vibration responses are measured at the tip of the smart beam via non-contact laser displacement meter. Laser displacement meter can operate in the range of +40 mm and -40 mm corresponding to +10 V and -10V.

A personal computer and LabVIEW are used for the implementation of active control. Multifunction

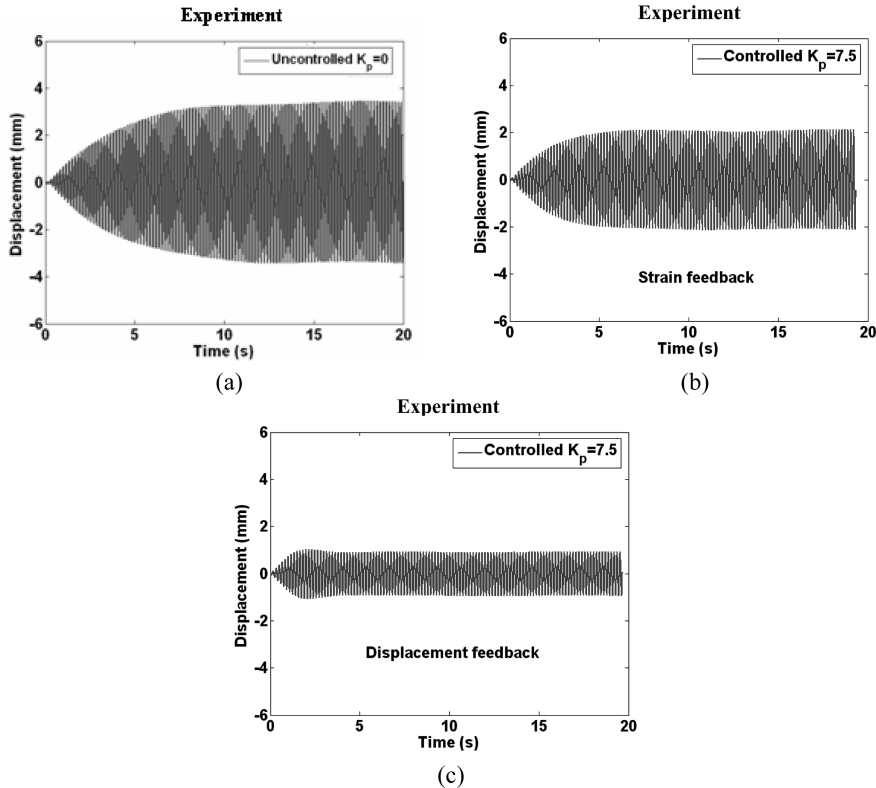


Fig. 7 Experimental results with sine wave of 6.12 Hz, (a) uncontrolled response, (b) controlled response with strain feedback for  $K_p=7.5$ , (c) controlled response with displacement feedback for  $K_p=7.5$

data acquisition cards are used to generate and acquire signals. Harmonic excitation that is a sine wave of 9V amplitude is created with PCI-6722 analog output card. The output signal amplified with the power amplifier is applied to the piezoelectric shaker. The amplifier gain is set as 30 during experiments. The response signal is recorded with PCI-6220 analog input card. For the active vibration control, the feedback signal is obtained with the analog input card and is subtracted from the reference value. The reference value is taken as zero so that the vibrations are eliminated at the tip of the beam. The control signal is calculated and sent to the power amplifier via the analog output card. The control signal sent by the analog output card is in the range of -9 V to 9 V. The parameters and controller gains employed in the experiments are the same as the simulation. Active control is achieved with both strain and displacement feedback. The uncontrolled and controlled vibration responses obtained by the experiment are shown in Fig. 7 (See Fig. 5 for the simulation results).

### 3. Simulation and experimental results

Experimental natural frequencies are found by applying a chirp signal to the piezoelectric shaker. The frequency of the chirp signal changes from 0.1 Hz to 110 Hz in order to determine the first three natural frequencies of the smart beam. The comparison of the experimental natural frequencies with the simulation results are given in Table 3.

Table 3 Natural frequencies of the smart beam

Method	Frequency (Hz)		
	1.	2.	3.
Simulation	6.129	36.604	106.500
Experiment	6.128	35.122	103.618

Control performances with the two feedback signals are tested for the controller gain values of  $k_p = 3.75$  and  $k_p = 15$ . Vibration responses are obtained with both the simulation and the experiment. The control action is started at  $t = 0$  s in order to decrease steady state vibration amplitudes of the smart beam under harmonic excitation. Actuation voltages become higher if the control actions start in any time after the excitation is applied. The maximum applicable amplitude of the actuation voltage is 270 V due to the experimental limitations.

### 3.1. Strain feedback control

Strain feedback signals are evaluated for the vibration reduction. Simulation and experimental results obtained with strain feedback control are shown in Fig. 8. The results include the uncontrolled and controlled responses for two different gain values. For the uncontrolled response, the transient parts in the simulation and experiment take approximately 7 s and 9 s, respectively. For the controlled responses,

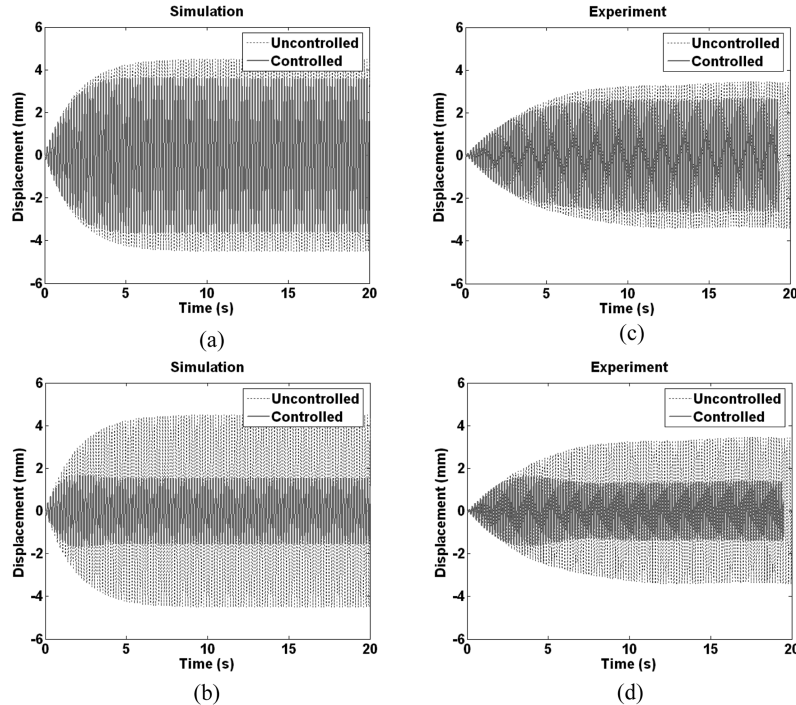


Fig. 8 For sine excitation at 6.12 Hz, uncontrolled and controlled vibration responses with strain feedback control, simulation for (a)  $K_p=3.75$  and (b)  $K_p=15$ , experiment for (c)  $K_p=3.75$ , (d)  $K_p=15$

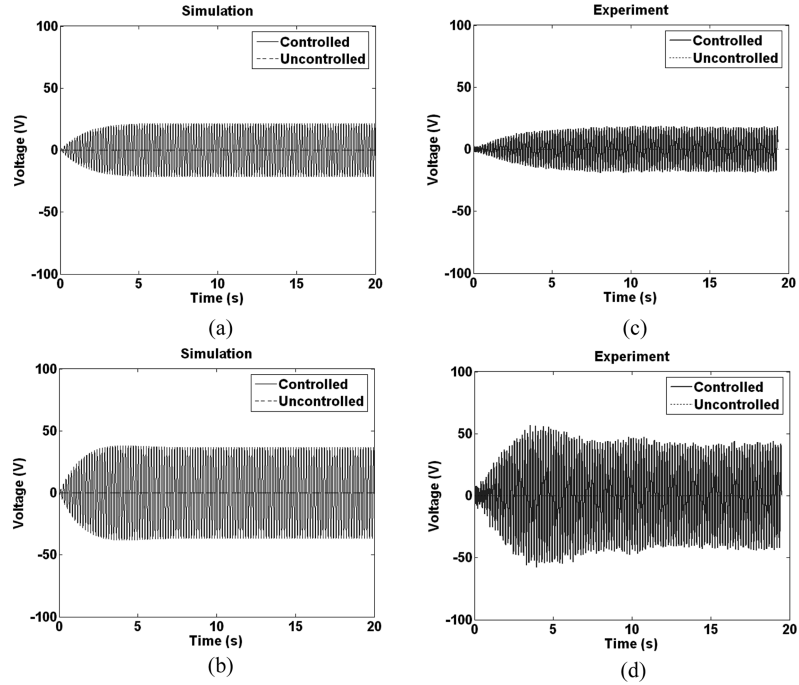


Fig. 9 Actuation voltages corresponding to the cases in Fig. 8, simulation for  $K_p=3.75$  and (b)  $K_p=15$ , experiment for (c)  $K_p=3.75$  and (d)  $K_p=15$

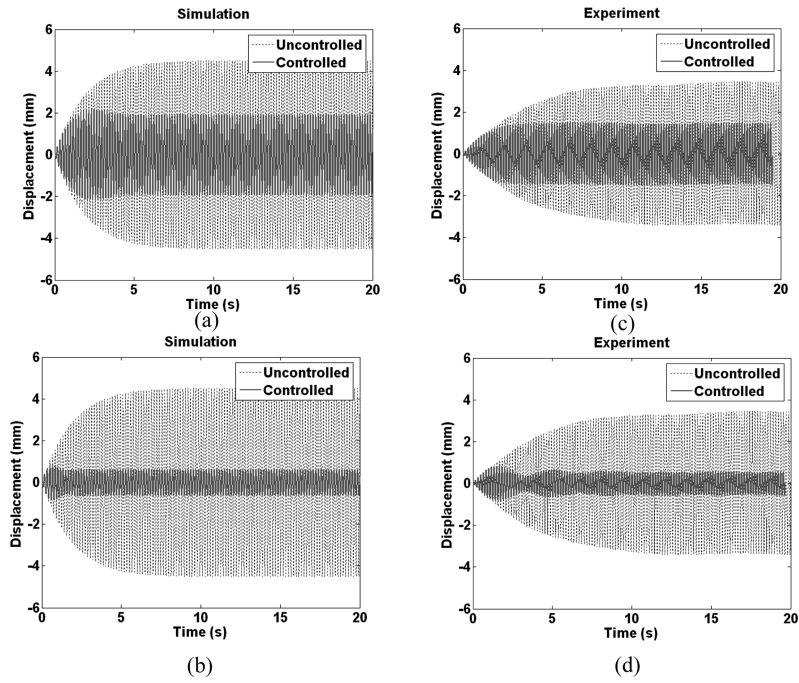


Fig. 10 For sine excitation at 6.12 Hz, uncontrolled and controlled vibration responses with displacement feedback control, simulation for (a)  $K_p=3.75$  and (b)  $K_p=15$ , experiment for (c)  $K_p=3.75$  and (d)  $K_p=15$

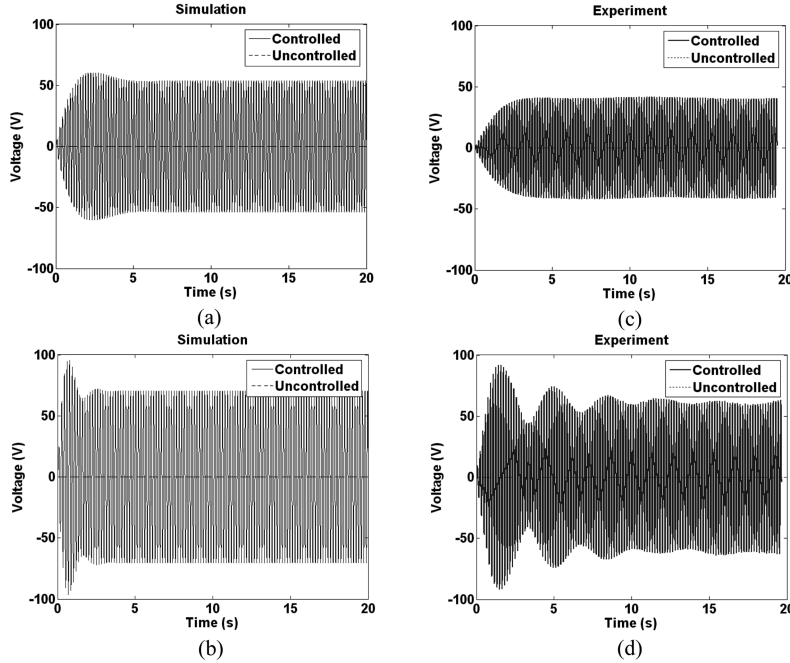


Fig. 11 Actuation voltages corresponding to the cases in Fig. 10, simulation for (a)  $K_p=3.75$  and (b)  $K_p=15$ , experiment for (c)  $K_p=3.75$  and (d)  $K_p=15$

higher gain provides better reduction in the amplitudes. Thus, Figs. 8(b) and (d) show 63% (simulation) and 61.5% (experimental) reduction in steady-state vibration amplitudes, respectively. Damping coefficients assumed in the simulation affect vibration amplitudes. Actuation voltages are shown in Fig. 9. The actuation voltages increase in Figs. 9(b) and (d) when the gain increases.

### 3.2. Displacement feedback control

Vibration reduction is also achieved with displacement feedback control. Fig. 10 shows the simulation and the experimental results with the same gains used in strain feedback control. Figs. 10(b) and (d) show 87% (simulation) and 85% reduction (experimental) in steady-state vibration amplitudes, respectively. Actuation voltages are shown in Fig. 11.

## 4. Conclusions

Direct control simulation using commercial FEA software ANSYS was realized by the authors in their previous study. In this study, active vibration control of smart beams excited harmonically is considered. Displacement and strain feedback are studied. Experimental results are also given.

It is observed that steady state vibration amplitudes can be reduced with the two feedback controls. Strain feedback control provides 63% (simulation) and 61.5% (experimental) reduction for steady-state vibration amplitudes. Displacement feedback control provides 87% (simulation) and 85% (experimental) reduction for steady-state vibration amplitudes. The reason for this result may be because the laser

displacement meter is located at the tip of the beam and it will carry mostly the effect of the first mode. On the other hand, the strain gauge is located 25 mm away from the clamped end, and the strain signals may be affected also by higher modes although a low-pass filter is used. In terms of maximum actuation values, the strain feedback control requires 59 V (simulation) and 63 V (experimental); the displacement feedback control requires 95 V (simulation) and 92 V (experimental). In general, the vibration reduction is the primary concern and it can be concluded that the displacement feedback is more effective. However, if the energy consumption is primary concern then the strain feedback is more effective.

Direct control simulation using commercial FEA packages make the analysis of active vibration control in smart structures easier. This study may be extended to more complex smart structures under various loading conditions such as moving loads and random excitations. Active vibration control of multiple input-multiple output (MIMO) systems may also be studied in the future.

## Acknowledgements

The authors acknowledge Turkish Scientific and Research Council (TUBITAK) for the financial support (Project Number: 104M373).

## References

- ANSYS (2004), *ANSYS user manual*, ANSYS, Inc., Canonsburg, PA, USA, ([www.ansys.com](http://www.ansys.com)).
- Baillargeon, B. P. and Vel, S. S. (2005), "Active vibration suppression of sandwich beams using shear actuators: experiments and numerical simulations", *J. Intell. Mater. Sys. Struct.*, **16**, 517-530.
- Bruant, I., Coffignal, G., Lene, F. ad Verge, M. (2001), "Active control of beam structures with piezoelectric actuators and sensors: modeling and simulation", *Smart Mater. Struct.*, **10**, 404-408.
- Choi, S. B., Park, S. B. and Fukuda, T. (1998), "A proof of concept investigation on active vibration control of hybrid structures", *Mechatronics*, **8**, 673-689.
- Dong, X. J., Meng, G. and Peng, J. C. (2006), "Vibration control of piezoelectric smart structures based on system identification technique: Numerical simulation and experimental study", *J. Sound. Vib.*, **297**, 680-693.
- Fariborzi, F., Golnaraghi, M. F. and Heppler, G. R. (1997), "Experimental control of free and forced structural vibration using a linear coupling strategy", *Smart Mater. Struct.*, **6**, 540-548.
- Gabbert, U., Trajkov, T. M. and Köppe, H. (2002), "Modelling, control and simulation of piezoelectric smart structures using finite element method and optimal control", *Mechanics, Automatic Control and Robotics*, **3**, 417-430.
- Jha, R. and Rower, J. (2002), "Experimental investigation of active vibration control using neural networks and piezoelectric actuators", *Smart Mater. Struct.*, **11**, 115-121.
- Karagüller, H., Malgaca, L. and Öktem, H. F. (2004), "Analysis by active vibration control in smart structures by ANSYS", *Smart Mater. Struct.*, **13**, 661-667.
- Kumar, R. and Singh, S. P. (2006), "Adaptive hybrid control of smart structures subjected to multiple disturbances", *Smart Mater. Struct.*, **15**, 1345-1357.
- Kusculuoglu, Z. K., Fallahi, B. and Roston, T. J. (2004), "Finite element model of a beam with a piezoceramic actuator", *J. Sound. Vib.*, **276**, 27-44.
- MATLAB (2004), The MathWorks, Inc., United States, [www.mathworks.com](http://www.mathworks.com).
- Meng, G., Yeb, L., Dong, X-J. and Wei, K. (2006), "Closed loop finite element modeling of piezoelectric smart structures", *Shock Vib.*, **13**, 1-12.
- Moita, J. M. S., Soares, C. M. M. and Soares, C. A. M. (2005), "Active control of forced vibrations in adaptive structures using a higher order model", *Smart Mater. Struct.*, **71**, 349-355.

- Peng, F., Ng, A. and Hu, Y. R. (2005), "Actuator placement optimization and adaptive vibration control of plate smart structures", *J. Intell. Mater. Sys. Struct.*, **16**, 263-271.
- Preumont, A. (2002), *Vibration control of active structures an introduction*, (2<sup>th</sup> ed.). Netherlands: Kluwer Academic Publishers.
- Reaves, C. M. and Horta, L. G. (2003), Piezoelectric actuator modeling using MSC/NASTRAN and MATLAB. *NASA/TM-2003-212651*, Langley Research Center, Hampton, Virginia.
- Raja, S., Prathap, G. and Sihna, P. K. (2002), "Active vibration control of composite sandwich beams with piezoelectric extension-bending and shear actuators", *Smart Mater. Struct.*, **11**, 63-71.
- Seba, B., Ni, J. and Lohmann, B. (2006), "Vibration attenuation using a piezoelectric shunt circuit based on finite element method analysis", *Smart Mater. Struct.*, **15**, 509-517.
- Xu, S. X., Koko, T. S. (2004), "Finite element analysis and design of actively controlled piezoelectric smart structures", *Finite Elements in Analysis and Design*, **40**, 241-262.
- Yaman, Y., Ülker, F. D., Nalbantoglu, V., Çalışkan, T., Prasad E., Waechter, D. and Yan, B. (2003), "Application of  $\mu$  synthesis active vibration control technique to a smart fin", *6<sup>th</sup> CanSmart Workshop* 109-119, Canada.
- Yang, S. M., Sheu, G. J. and Liu, K. C. (2005), "Vibration control of composite smart structures by feedforward adaptive filter in digital signal processor", *J. Intell. Mater. Sys. Struct.*, **16**, 773-779.

CC